FISEVIER

Contents lists available at ScienceDirect

Geomechanics for Energy and the Environment

journal homepage: www.elsevier.com/locate/gete



Forecasting and mitigating landslide collapse by fusing physics-based and data-driven approaches



Carolina Seguí a,*, Manolis Veveakis b

- a RWTH Aachen University, Aachen, Germany
- ^b Duke University, Durham, NC, USA

ARTICLE INFO

Article history:
Received 4 September 2022
Received in revised form 23 October 2022
Accepted 23 October 2022
Available online 2 November 2022

Editors-in-Chief: Professor Lyesse Laloui and Professor Tomasz Hueckel

Keywords: Basal temperature Landslide monitoring Stability analysis Early warning Forecasting collapse

ABSTRACT

Deep-seated landslides represent one of the most devastating natural hazards on earth, typically creeping at inappreciable velocities over several years before collapsing at catastrophic speeds. They can have detrimental consequences to society, causing fatalities and prone to affect transportation infrastructures. Currently, limited data-driven tools allow a time-dependent assessment of these landslides, mainly linking their motion with groundwater variations or forecasting the collapse time using the empirical inverse velocity-time approach. In this study, we validate that monitoring the basal temperature of a creeping landslide, and fusing it with physics-based modeling, can offer predictive and control capabilities for the landslide's response. By following the theoretical suggestions of several works, we installed a thermometer on the sliding surface of a creeping landslide in Andorra. In this paper, we report the results of 3 months of recording and identify the basal stress-temperature space as the underlying unobserved phase space that determines the problem and allows us to forecast and control the landslide. Following our results, we validate our suggestion by applying the model to three other cases, where temperature measurements are unavailable: the Vajont (Italy) and Mud Creek (California) collapsed landslides and the active Shuping landslide (China). The study shows that physics-based models can be trained in the same phase space and offer forecasting and control capabilities. We anticipate our results to be the starting point for a new era in monitoring, controlling, and forecasting deep-seated landslides, aiming at alleviating their devastating impact on society.

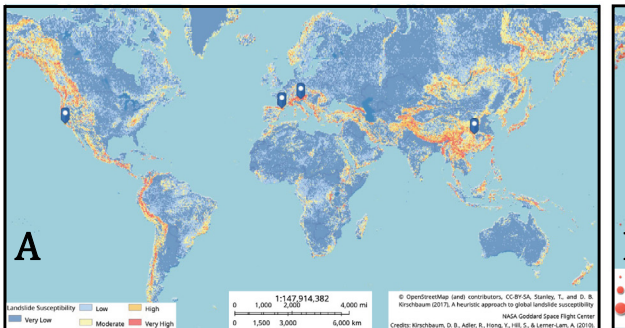
© 2022 Elsevier Ltd. All rights reserved.

1. Introduction

Deep-seated landslides are sizeable slides involving millions of cubic meters of soil moving as a rigid block on top of a deep (below the roots of the trees and the groundwater level) basal layer of heavily deformed minerals. These landslides shear as translational/rotational (depending on the stratigraphy of the area), with very low velocities (cm/year) during long periods (years to tens of years). However, their collapse is usually very sudden, happening within minutes and without previous warning, reaching high velocities, 1,2 as high as the 120 m/s reported at the 1963 Vajont landslide in Italy.3 The catastrophic and fast collapse of this kind of landslide makes the evacuation of the area that could be affected almost impossible, thereby possibly causing fatalities and infrastructure damages.^{3–7} Moreover, the lack of understanding of the physical processes behind the mechanisms of failure of this kind of landslide makes the development of reliable, data-driven, early warning systems (or tools/protocols to stop the acceleration of the landslide) challenging, therefore potentially causing significant damages to civil infrastructures. As shown in Fig. 1A, the landslide-prone areas spread worldwide, having a detrimental fatality rate (Fig. 1B). This figure highlights that landslides are a globally threatening natural hazard with incommensurate consequences.

A notable example of disproportionate consequences is the case of the 1963 Vajont landslide in Northeastern Italy, which is among the top human-related catastrophes in history, 11 with almost 2000 fatalities and unprecedented infrastructure damage.³ Since the landslide collapsed in 1963, several studies have presented different mechanisms involved as triggering factors of the acceleration and final collapse of deep-seated landslides, such as groundwater variations. 12,13 Some models tried to forward predict the catastrophic collapse of a landslide by, for example, inverting the field velocity data until it reaches zero or its displacement goes to infinity.^{2,14,15} However, these models are predominantly phenomenological and data-driven, thus not accounting for additional information considered the key to the problem. Such physics-based input includes the characterization and response of the material deforming inside the sliding surface (shear band), being the most critical part of a deep-seated landslide, and where all the physical-mechanical processes that

^{*} Corresponding author. E-mail address: segui@gut.rwth-aachen.de (C. Seguí).



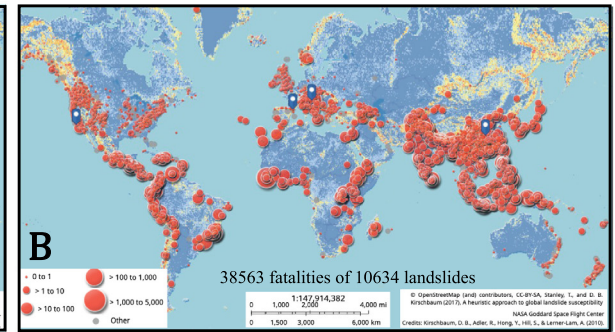


Fig. 1. Global impact of landslides. **A.** World map of landslide susceptibility, highlighting areas prone to landslides with a color scale, from blue as the lower susceptible to red as the highest one. The four pins correspond to the locations of the four deep-seated landslides discussed in this work. **B.** Map of fatalities from landslides worldwide between 1956–2020 (last access July 2020). The data for this figure was collected from NASA's Cooperative Open Online Landslide Repository (COOLR).^{8–10} The red dots represent the landslides that have collapsed and their size represents the range of fatalities that each one has caused. Highlighted in blue are the four case studies that we present in this study: the El Forn landslide (Andorra), the Vajont landslide (Italy), the Shuping landslide (Three Gorges Dam, China), and the Mud Creek landslide (California, USA).

determine the evolution of the landslide are operating. ¹⁶ Hence, it is imperative to seek more answers on the behavior of a deep-seated landslide by attempting to enrich our data-driven capabilities with physics-based constraints stemming from the response of the shear band material to external loading.

It has been seen in monitored landslides that external factors, such as the variations of groundwater, trigger the movement of the landslide. 12,17 These groundwater variations usually depend on seasonal/heavy rainfall (such as the Mud Creek landslide), snow melting (such as the El Forn landslide), or a nearby dam (such as the Vajont and Shuping landslides). Moreover, other studies 18-26 show that adding internal factors in the model of a deep-seated landslide, such as material properties of the shear band, constrain triggering factors of the behavior of a deep-seated landslide and follow its accelerations during its creeping phase until its final collapse. Most deep-seated landslides present a shear band formed by clay or clay-like materials, which can be thermal and velocity-sensitive 27,28 when the material experiences changes in pressure and is sheared, thus facilitating the acceleration of the landslide.

The present model intends to include the physical parameters of the shear band (material's properties), also accounting for the thermal and velocity sensitivities of the shear band's material, and the external factors of the landslide such as the groundwater variations in time. For this reason, it is difficult to add all the physical mechanisms operating in the landslide's shear band and, therefore, how to evaluate these parameters, considering the unavailability to access shear band material. For this reason, we suggest a method of fusing a physics-based model with data-driven parameter constrain by using an energy-based mathematical model in a reduced and dimensionless form (that depends on a single dimensionless parameter that can be constrained by the data).^{26,28} The model is described in the Methods section and includes a single dimensionless parameter, the Gruntfest number²⁹ Gr, expressing the ratio of the mechanical work converted into heat over the heat diffusion capabilities of the shear-band material (Eq. (5)). The Gruntfest number includes all the material properties at hand (thermal conductivity, rate and thermal sensitivities, and reference rate),²⁷ as well as the thickness of the shear band and the loading shear stress (applied on the shear band from the external loading sources, such as gravity and groundwater).^{26,28} In the absence of detailed information on the material, this dimensionless parameter can be used as a free parameter and be constrained by available data.²⁸

This study applies the mathematical model, presented previously by the authors, ^{21,26,28} incorporating four landslides: the Vajont (Italy) and Mud Creek (California, USA) landslides that

collapsed, and the Shuping (Three Gorges Dam, China) and El Forn (Andorra) landslides that remain active. The aim of this paper is to show that the stability analysis and the mathematical model can be applied to different case studies, that either collapse or remain active, in the same phase space and give critical values of measurable properties (i.e., pore water pressure, basal temperature). The model uses a phase space to represent the behavior of the landslide, in terms of temperature and Gruntfest number (i.e., external loading), allowing us to see all possible states of the system of equations of the mathematical model. The results of the calculated values of temperature and Gruntfest number, for each groundwater level, are represented in unique points inside the phase space. Each of these landslides presented have been studied with different data available: Shuping and Mud Creek with velocity and shear stress, Vajont with velocity, shear stress, and some material parameters, and El Forn with velocity, pore pressure, basal temperature, and material properties from the shear band obtained in the laboratory. The importance of considering the basal temperature, the material properties of the shear band, and the external loading for all the landslides can give estimations of when the landslide will become unstable and collapse catastrophically by using the same phase space and the same variables for all the landslides. Moreover, this study shows that the stability analysis can be performed with this mathematical model and implemented in the phase space without having information on the material of the shear band (i.e., purely data-driven).

2. Methods

2.1. Description of the mathematical model

The equations used in the mathematical model focus on the behavior of the material located inside the shear band, and assume that the material is at a critical state (deforming under constant volume), fully saturated in water, visco-plastic, and its mechanical properties vary along the vertical axis, z, of the shear band. 21,26,27

Using the arguments presented in detail by Rice, ³⁰ Veveakis et al., ²¹ Seguí et al., ²⁶ stress equilibrium inside the shear band $(\frac{\partial \sigma'_{XZ}}{\partial z} = \frac{\partial \sigma'_{ZZ}}{\partial z} = 0)$ yields constant profiles of the effective stresses inside the shear band and equal to their external values: $\sigma'_{XZ} = \tau_d(t)$ for the shear stress and $\sigma'_{ZZ} = \sigma'_n(t)$ the normal stress. Correspondingly, since the material is at a critical state (i.e. deforming under constant volume), the mass balance yields the incompressibility condition for zero volumetric strain rate $\dot{\epsilon}_V = \dot{\epsilon}_{ZZ} = 0$. Therefore, the main equation describing the

response of the basal material is the energy equation, ^{21,26,27,30} reading:

$$\frac{\partial T}{\partial t} = c_{th} \frac{\partial^2 T}{\partial z^2} + \frac{\tau_d \dot{\gamma}}{\rho C_m} \tag{1}$$

with boundary conditions $T=T_{boundary}$ at the boundaries of the shear band, $z=-\frac{ds}{2}$, $\frac{ds}{2}$ (ds is the thickness of the shear band). In this equation, ρC_m is the heat capacity of the shear band material and $c_{th}=jk_m/\rho C_m$ is the thermal diffusivity, and jk_m being the thermal conductivity.

The shear band material is assumed to be visco-plastic, thus, defining the strain rate at critical state as a combination of velocity hardening and thermal softening of the clayey material²⁷ as follows:

$$\dot{\gamma} = \frac{\partial V}{\partial z} = \dot{\gamma}_{ref} \left(\frac{\tau_d}{\tau_{ref}} \right)^{1/N} e^{m(T - T_{boundary})}, \quad m = \frac{M}{N}$$
 (2)

being τ_d the shear stress of the landslide evolving in time, τ_{ref} a reference shear stress of the landslide, $\dot{\gamma}_{ref}$ a reference strain rate, m is the ratio of thermal and rate sensitivity of the material, with M the thermal sensitivity and N the rate sensitivity of the shear band's material. 21,26,27

Following all these considerations, Eq. (1) can be combined with Eq. (2), and further be reduced to a single parameter dimensionless equation

$$\frac{\partial \theta^*}{\partial t^*} = \frac{\partial^2 \theta^*}{\partial z^{*2}} + Gr e^{\theta^*}, \ z^* \epsilon [-1, 1], \ t > 0$$
 (3)

where the following dimensionless parameters have been used:

$$z^* = \frac{z}{\left(\frac{ds}{2}\right)}, \ t^* = \frac{c_{th}}{\left(\frac{ds}{2}\right)^2}t, \ \theta^* = m(T - T_{boundary})$$
 (4)

The dimensionless group, *Gr*, the so-called Gruntfest number, ²⁹ has a base value defined as:

$$G_0 = m \frac{\tau_{ref} \dot{\gamma}_{ref}}{jk_m} \left(\frac{ds}{2}\right)^2 \left(\frac{\tau_d}{\tau_{ref}}\right)^{1+1/N} \tag{5}$$

Note that the velocity is calculated from Eq. (2), through integration inside the shear band.

2.2. Calculation of the model's phase space

By performing a bifurcation analysis using an arc-length continuation algorithm²⁶ on the steady-state of Eq. (3), we obtain the bifurcation diagram (phase space) of Fig. 2A. The model has 2, 1, or no steady solutions depending on the value of Gr: For $Gr < Gr_c$, the equation has two steady solutions (Fig. 2B), a stable (lower branch) and an unstable (upper branch). Any initial condition inside the highlighted gray area will lead the system to the stable branch (Fig. 2C) and any initial condition outside will lead the system to a blow-up instability (Fig. 2D); For $Gr = Gr_c$ the system has one, saddle point solution (Fig. 2B); For $Gr > Gr_c$ the system has no steady-state solutions and any initial condition in this area will blow-up (Fig. 2B).

2.3. Using water pressure as input data

To fully characterize the dependence of the shear stress, τ_d , on the groundwater pressure and its variations, a regional hydrogeo-mechanical model is required. However, in two of the cases under consideration, the El Forn and Mud Creek landslide, such an analysis cannot be easily performed since the landslides are either fed/loaded from the pressure changes of the groundwater below the shear band (El Forn), or the sliding surface location was unknown (Mud Creek). These challenges are, in turn, not

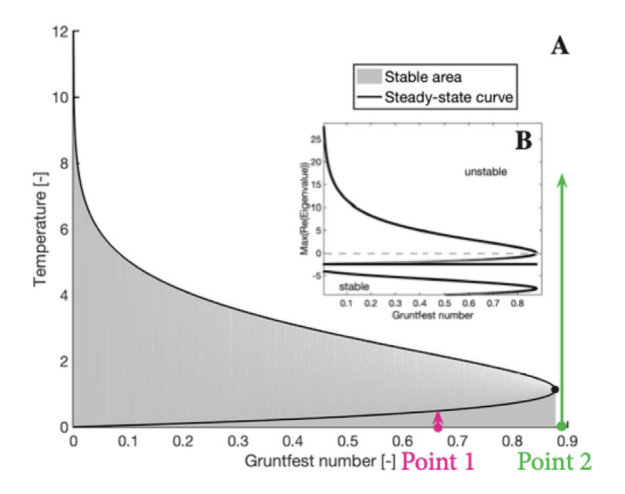
allowing us to determine the shear stresses through modeling approaches. To overcome these challenges, we will hereby use the outcomes of the hydro-geo-mechanical analysis of Seguí et al., ²⁶ suggesting that the shear stress, τ_d , varies linearly with the water pressure, p_f , recorded in the vicinity of the shear band. We have therefore set the shear stress to be directly proportional to the (pore) pressure, $\tau_d = \tau_{d,ref}(p_f/p_{f0})$, where $\tau_{d,ref}$ is a -currently unspecified- reference value of the shear stress applied on the shear band, when the fluid pressure is at the reference value, p_{f0} . Through this definition, the pore pressure data are used as a loading input on the Gruntfest number, Gr, and will be further constrained through the available data.

2.4. Stability analysis

By therefore studying the stability of the heat energy-based equation (Eq. (3)), we obtain a phase space of the model by plotting the Gruntfest number against the basal temperature (Fig. 2A). This phase space is delimited by a black line in Fig. 2A and indicates the area of stability of the landslide. While the basal temperature and Gruntfest remain within the stable area of the phase space (gray area of Fig. 2A), the landslide remains in a stable creeping regime. In the creeping regime, the landslide reacts to changes in the shear band's temperature and changes in the external loading stresses (i.e., groundwater level variations). As soon as the basal temperature and Gruntfest transition to the unstable area of the phase space (white area of Fig. 2A), the landslide becomes unstable and accelerates catastrophically, without any response to remediation actions.²⁶ The physics of the model are, therefore, giving critical values of temperature and loading stress (i.e., Gruntfest). These results allow us to forecast when the landslide will turn unstable and collapse catastrophically, as long as the "typically unobservable" fields of (dimensionless) basal temperature and shear stress can be measured or inferred by the observable quantities of the collected data (typically displacement/velocity and groundwater pore pressure).

3. Results and discussion

In this study, we test the applicability of the aforementioned physics-based model²⁶ on data from four deep-seated landslides: the Vajont landslide (in Italy)²⁶ and the Mud Creek landslide (in California, USA), both of which collapsed catastrophically after prolonged creeping phases; the currently active Shuping landslide (in the Three Gorges Dam, China); and the El Forn landslide (Andorra).²⁸ We first showcase the validity of the theoretical phase space by presenting the results of monitoring the temperature of an active deep-seated landslide.²⁸ The El Forn landslide was instrumented with a thermometer in the shear band, and four months of recording data are shown in Fig. 3A, along with the groundwater pressure.²⁸ The data show that the thermal response of the shear band directly depends on the water pressure. By using in the model, the monitored field temperature from the shear band and the field water pore pressure from the installed piezometer, we can calculate the temperature inside the shear band by using Eq. (3). The calculated temperature of the shear band in our model, allows us to reproduce the field temperature by tuning the base value of the Gruntfest number (Eq. (5)), G_0 , found as the value that best fits the field temperature. Having constrained the single parameter of the model, G_0 , we can now forecast the velocity/displacement of the landslide from Eq. (3), as shown in Fig. 3B. Finally, once the data have been used to calibrate the model, we can map the temperature/normalized velocity and the Gruntfest/shear stress/(pore) pressure data of the landslide on the phase space of the model (see Methods section),



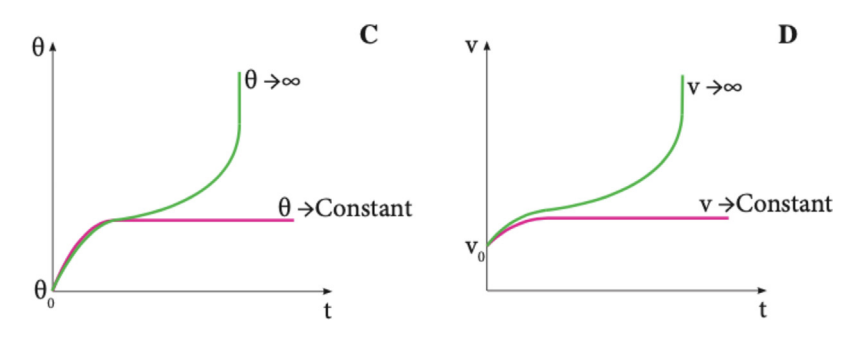


Fig. 2. Bifurcation diagram for the stability of the landslide. **A.** Steady-state curve with its critical point (black dot), and the corresponding maximum eigenvalue (inset B). **B.** A stable point 1 (pink dot), and an unstable point 2 (green point) are highlighted. The pink and green arrows represent the evolution in time of the system with an initial state described by points 1 and 2 respectively. **C.** Representation of the temperature evolution in time starting from the stable and unstable points from Fig. 2A. **D.** Representation of the velocity evolution in time starting from the stable and unstable points from Fig. 2A.

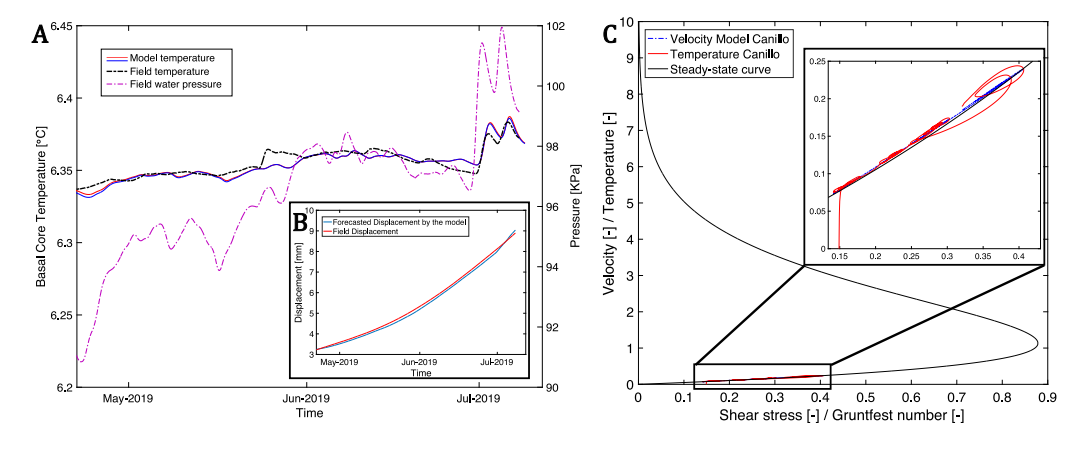


Fig. 3. Forecasting and controlling the response of the El Forn landslide. A. Temperature and water pressure field data with the calculated temperature in our model. The field data show that pressure variations indeed affect the temperature of the material (at high precision, as the difference in temperature values could be considered almost negligible) and follow the same behavior as the water pressure. The temperature calculated in the model shows that indeed, the model can reproduce with accuracy the response of the temperature. B. Field displacement data with the forecasted displacement calculated in our model from the temperature calculated. C. Phase space mapping the field temperature data with the Gruntfest number calculated (in red) and the velocity calculated in the model with the field shear stress (pore pressure). We observe that both the field and the model's data follow the model's phase space, thus suggesting that the "unobservable variable" or temperature space could be used to train the model and forecast the landslide's "observable" motion.

as shown in Fig. 3C. We observe that the field data (temperature and pore pressure/shear stress) and the calculated data as Gruntfest and velocity follow the phase space suggested by the model. In a recent paper, ²⁸ the authors obtained the input parameters of the model for this landslide from laboratory experiments on the shear band's material, confirming the validity of the inverted values of the Gruntfest number.

Having validated the feasibility of the physics-based model through monitoring the basal temperature of an active landslide²⁶ (Fig. 3), we will explore in the next steps if the physics-based model can be equally used without having detailed information about the basal temperature and the material's parameters. To this end, we will apply the model to the Mud Creek landslide, which catastrophically collapsed on May 20th of 2017, after years of creeping.³¹ The only available data are the velocity obtained

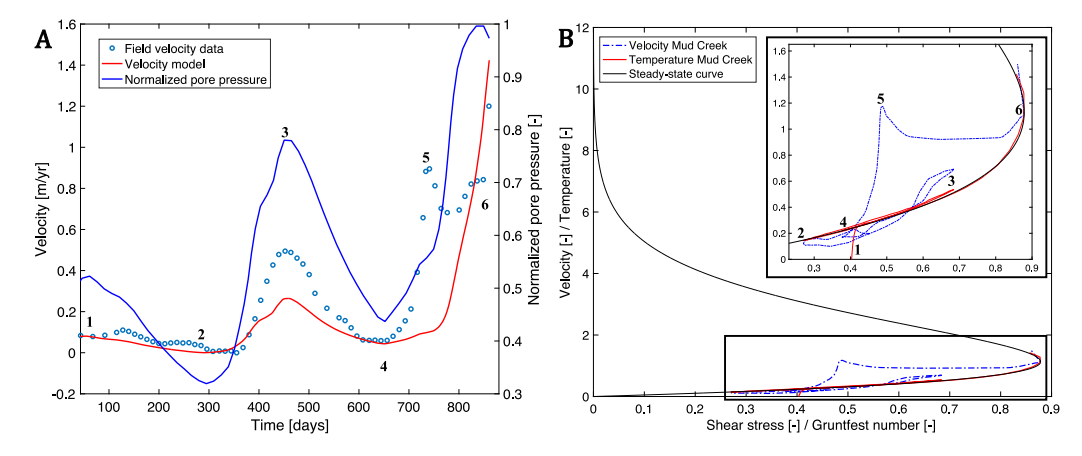


Fig. 4. Forecasting and controlling the response of the Mud Creek landslide. **A.** Pore pressure (blue line) and velocity data (blue dots) from,³¹ with the velocity calculated in our model (red line). **B.** Basal temperature and Gruntfest number calculated in our model mapped in the phase space, as well as the field velocity and pore pressure (shear stress). The inset shows a zoom of the field and calculated data behavior in the phase space with numbers correlating the data shown in Fig. 4A, showing the point when the landslide turns unstable and collapses catastrophically.

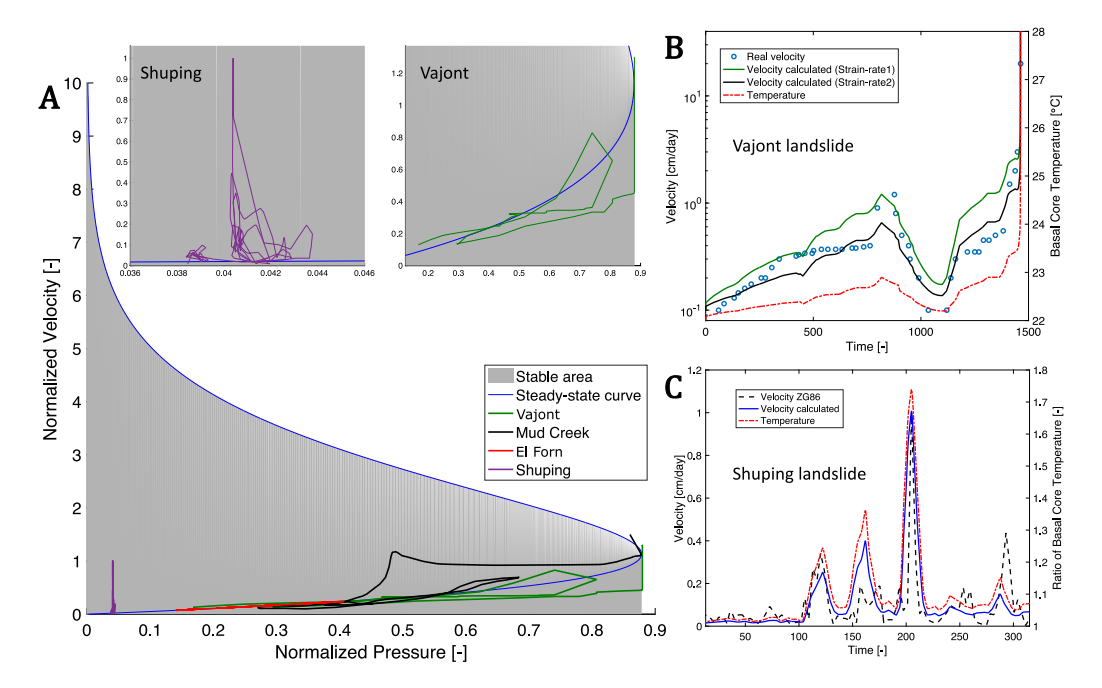


Fig. 5. Controlling deep-seated landslides through basal temperature. A. Mapping of the calculated loading pressures and velocities of the four landslides on the phase space of the model's response. We observe that all four landslides follow the model's phase space, with the Vajont and the Mud Creek collapsing catastrophically when exceeding the stable (gray) area of the model, and the El Forn and Shuping inside the stable area of the phase space. It is therefore suggested that deep-seated landslides can be controlled by maintaining their pressure and temperature inside the gray area of this phase space. The insets show a zoom of the Shuping and Vajont landslides in the phase space. B. The Vajont landslide field velocity with the calculated velocities and basal temperature. As the velocity and temperature behavior show, once the phase space (Fig. 5A) is exceeded, both variables (velocity and temperature) increase infinitely, thus, a catastrophic collapse occurs. C. The Shuping landslide field velocity, with the calculated velocity and basal temperature. It is shown in Fig. 5A, that this landslide is still very stable, regardless of the variations of groundwater pressure and temperature experienced until the end of this data period.

from satellite imaging of the area and the normalized pore pressure inferred from the precipitation data³¹ (Fig. 4A). Using the pore pressure as the driving loading factor (see Methods section) and calibrating the value of the Gruntfest number required for the model to follow the phase space, we retrieve that the landslide collapses during the last decrease of the pore pressure. Fig. 4A shows the data of the pore pressure and the velocity, with the forecasted velocity from our model. In Fig. 4B, we show that by using the velocity and pore pressure data (shear stress) and calibrating the physics-based model on its phase space, we can adequately reproduce the history of the Mud-Creek slide without any knowledge of the basal material. The results of the field and

calculated data of the Mud Creek landslide follow the stable area of the phase space (lower branch of the steady-state curve) until the (pore) pressure/Gruntfest and velocity/basal temperature reach the stable threshold, therefore entering the tertiary creep of the landslide and its catastrophic collapse.

Moreover, the model is applied to the Shuping and Vajont landslides.²⁶ These two landslides have similar geometry and material of the shear band (clays) and are ancient landslides reactivated upon the construction of a dam in their vicinity. Thus, both landslides' behavior depends directly on the pore pressure variations caused by the dam's operations (Fig. 5B, C). The Vajont landslide collapsed catastrophically while the Shuping landslide

remains actively creeping. The results of the transient model applied to the two case studies show that, indeed, the model can be trained on its phase space and be used to forecast the evolution and stability of the landslide (Fig. 5A), without deep knowledge of the material's properties.

4. Conclusions

Summarizing the importance of the phase space in landslide forecasting and control, Fig. 5A shows the response of all landslides in the observed velocity-pressure phase space calculated from the unobserved temperature-Gruntfest number phase space. Fig. 5A suggests that regardless of the size and characteristics of each landslide and its shear band material, all landslides can be mapped in the same phase space, whether they remain active or already collapsed. These results suggest that temperature is a key factor in the behavior of a deep-seated landslide. Adding the basal temperature in the model to forecast a landslide behavior has been previously discussed and proved by the authors.²⁸ Thus, monitoring the temperature in the shear band of the landslide and implementing the presented model in real time allows us to forecast and control the behavior of the landslide, even with limited knowledge of the shear band's material. This new model, thus, allows the engineers in charge to take remediation measures while the landslide is stable and prevents catastrophic acceleration.

CRediT authorship contribution statement

Carolina Seguí: Data curation, Writing – original draft, Investigation, Formal analysis, Methodology, Validation, Reviewing and editing. **Manolis Veveakis:** Supervision, Methodology, Conceptualization, Reviewing and editing, Project administration, Funding acquisition.

Declaration of competing interest

The authors declare that they have no known competing financial interests or personal relationships that could have appeared to influence the work reported in this paper.

Data availability

Data will be made available on request.

Acknowledgments

The authors would like to acknowledge Xavier Planas from the Government of Andorra to provide us with the core samples of the landslide and the field data, and Jose Moya from BarcelonaTech University to provide us with the field data. This work was supported by the National Science Foundation, USA [CMMI-2006150].

References

- 1. Smalley IJ. Rockslides and avalanches. Nature. 1978;272(5654):654.
- Voight Barry. A method for prediction of volcanic eruptions. Nature. 1988;332(6160):125–130.
- Mueller L. The rock slide in the vaiont valley. Felsmech Ingenieurgeol. 1964;2:148–212.

- Preisig Giona. Long-term effects of deep-seated landslides on transportation infrastructure: a case study from the Swiss Jura mountains. Q J Eng Geol Hydrogeol. 2019;52(3):326–335.
- Chang Kuo-Jen, Taboada Alfredo. Discrete element simulation of the Jiufengershan rock-and-soil avalanche triggered by the 1999 Chi-Chi earthquake, Taiwan. J Geophys Res Earth Surf. 2009;114(F3).
- Huang C, Chen M, Hsu M. A preliminary report on the chiufenershan landslide triggered by the 921 Chi-Chi earthquake in Nantou, central Taiwan. Terr Atmos Ocean Sci. 2002;T13:387–395.
- 7. Wang W, Chigira M, Furuya T. Geological and geomorphological precursors of the chiu-feng-erh-shan landslide triggered by the Chi-Chi earthquake in central Taiwan. *Eng Geol.* 2003;69:1–13.
- Juang CS, Stanley TA, Kirschbaum DB. Using citizen science to expand the global map of landslides: Introducing the cooperative open online landslide repository (COOLR). PLoS One. 2019;14(7):e0218657.
- Kirschbaum Dalia, Stanley Thomas, Zhou Yaping. Spatial and temporal analysis of a global landslide catalog. *Geomorphology*. 2015;249:4–15. Geohazard Databases: Concepts, Development, Applications.
- Kirschbaum DB, Adler R, Hong Y, Hill S, Lerner-Lam A. A global landslide catalog for hazard applications: method, results, and limitations. *Nat Hazards*. 2010;52:561–575.
- UNESCO. International year of planet earth global launch event 12-13 february 2008. 2008.
- 12. Terzaghi Karl. Mechanism of landslides. In: Application of Geology to Engineering Practice. Geological Society of America; 1950:83–123.
- Iverson RM, Major JJ. Rainfall, ground-water flow, and seasonal movement at Minor Creek landslide, northwestern California: physical interpretation of empirical relations. 1987;99(4):579–94.
- Saito M. Forecasting the time of occurrence of a slope failure. In: Proc. 6th Int. Conf. on Soil Mechanics and Foundation Engineering, Montreal, Vol. 1. 1965:537–541
- Saito M. Forecasting time of slope failure by tertiary creep. In: Proc. 7th Int. Conf. on Soil Mechanics and Foundation Engineering, Mexico, Vol. 2. 1965:419–445.
- Gonzalez de Vallejo Luis I, Ferrer Mercedes. Geological Engineering. Leiden, The Netherlands: CRC Press/Balkema; 2011.
- 17. Terzaghi K. Theoretical Soil Mechanics. New York: John Wiley and Sons; 1943.
- Vardoulakis I. Catastrophic landslides due to frictional heating of the failure plane. Mech Cohes Frict Mater. 2000;5:443–467.
- Vardoulakis I. Dynamic thermo-poro-mechanical analysis of catastrophic landslides. *Geotechnique*, 2002;52:157–171.
- Chang K, Taboada A, Lin M, Chen R. Analysis of landsliding by earthquake shaking using a block-on-slope thermo-mechanical model: Example of Jiufengershan landslide, central Taiwan. Eng Geol. 2005;80:151–163.
- Veveakis E, Vardoulakis I, DiToro G. Thermoporomechanics of creeping landslides: The 1963 vaiont slide, northern Italy. J Geophys Res. 2007:112:F03026.
- 22. Goren L, Aharonov E. Long runout landslides: The role of frictional heating and hydraulic diffusivity.. *Geophys Res Lett.* 2007;34:L07301.
- Regenauer-Lieb K, Yuen D, Fusseis F. Landslides, ice quakes, earthquakes: A thermodynamic approach to surface instabilities. *Pure Appl Geophys*. 2009;166(10-11):1885-1908.
- **24.** Goren L, Aharonov E, Anders MH. The long runout of the heart mountain landslide:Heating, pressurization, and carbonate decomposition. *J Geophys Res.* 2010;115:B10210.
- Cecinato Francesco, Zervos Antonis, Veveakis Emmanuil. A thermomechanical model for the catastrophic collapse of large landslides. Int J Numer Anal Methods Geomech. 2011;35(14):1507–1535.
- Seguí C, Rattez H, Veveakis M. On the stability of deep-seated landslides. The cases of vaiont (Italy) and shuping (three Gorges dam, China). J Geophys Res Earth Surf. 2020;125:e2019JF005203, e2019JF005203 2019JF005203.
- Vardoulakis I. Steady shear and thermal run-away in clayey gouges. Int J Solids Struct. 2002;39:3831–3844.
- Seguí Carolina, Veveakis Manolis. Continuous assessment of landslides by measuring their basal temperature. *Landslides*. 2021;18(12):3953–3961.
- Gruntfest I. Thermal feedback in liquid flow: Plane shear at constant stress. Trans Soc Rheol. 1963;7:95–207.
- Rice JR. Heating and weakening of faults during earthquake slip. J Geophys Res. 2006;111:B05311.
- 31. Handwerger Alexander L, Huang Mong-Han, Fielding Eric Jameson, Booth Adam M, Bürgmann Roland. A shift from drought to extreme rainfall drives a stable landslide to catastrophic failure. *Sci Rep.* 2019;9(1):1569.